

## Supporting Information

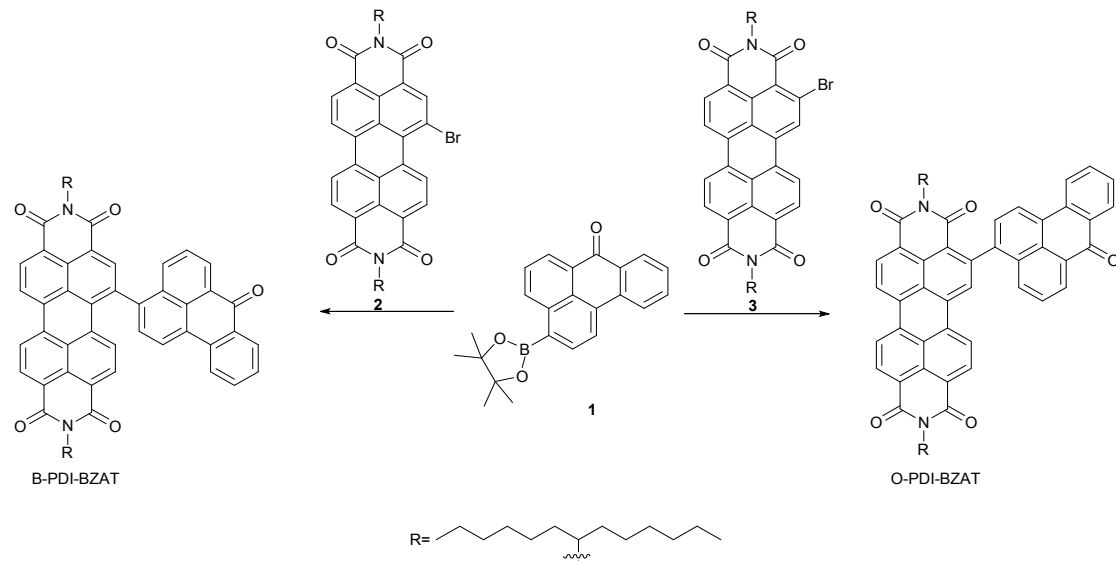
### Discovery and Insight into One-photon and Two-photon Excited ACQ-to-AIE Conversion via Positional Isomerization

Xuetong Long,<sup>a</sup> Jieyu Wu,<sup>b</sup> Sirui Yang,<sup>a</sup> Ziqi Deng,<sup>a</sup> Yusen Zheng,<sup>a</sup> Wenying Zhang,<sup>a</sup> Xiao-Fang Jiang,<sup>b</sup> Fushen Lu,<sup>a</sup> Ming-De Li,<sup>a</sup> Liang Xu,\*<sup>a</sup>

<sup>a</sup>Ms. X. Long, Ms. S. Yang, Mr. Z. Deng, Mr. Y. Zheng, Ms. W. Zhang, Prof. F. Lu, Prof. M. Li, Dr. L. Xu, Department of Chemistry and Key Laboratory for Preparation and Application of Ordered Structural Materials of Guangdong Province, Shantou University, Guangdong 515063, China, Email: xuliang@stu.edu.cn

<sup>b</sup>Ms. J. Wu, Prof. X. Jiang, Laboratory of Quantum Engineering and Quantum Material, School of Physics and Telecommunication Engineering, South China Normal University, Guangzhou 510006, China

#### 1. Synthesis



Scheme S1 The synthetic routes of B-PDI-BZAT and O-PDI-BZAT.

#### Synthesis of B-PDI-BZAT

Compound 1, 2 and 3 were synthesized according to the literature.<sup>1</sup> A mixture of 1 (1.72 g, 4.82 mmol), 2 (2.01 g, 2.41 mmol), Pd(PPh<sub>3</sub>)<sub>4</sub> (0.14 g, 0.12 mmol), K<sub>2</sub>CO<sub>3</sub> (0.67 g, 4.82 mmol), DMF (50 mL) was stirred at 80 °C under N<sub>2</sub> atmosphere for 24h. After cooling, DMF was removed by rotary evaporator. The residue was then purified by column chromatography (petroleum ether: DCM = 6:1 to 1:1). A dark red solid of B-PDI-BZAT (1.71 g, 1.74 mmol) was obtained in 72% yield. <sup>1</sup>H NMR (500 MHz, CDCl<sub>3</sub>) δ 8.81-8.74 (m, 3H), 8.70-8.68 (d, 2H), 8.64-8.62 (d, 2H), 8.58-8.56 (d, 1H), 8.45-8.43 (d, 1H), 8.07-8.05 (d, 1H), 7.88-7.82 (m, 2H), 7.79-7.78 (d, 1H), 7.69-7.61 (m, 3H), 5.19-5.04 (m, 2H), 2.25-2.12 (m, 4H), 1.86-1.76 (m, 4H), 1.33-1.16 (m, 32H), 0.84-0.77 (m, 12H). <sup>13</sup>C NMR

(125 MHz, CDCl<sub>3</sub>) δ 182.58, 141.68, 137.24, 134.61, 132.69, 130.85, 130.09, 129.59, 128.99, 128.26, 128.14, 128.11, 128.04, 127.96, 127.92, 127.34, 126.86, 126.81, 126.26, 126.18, 123.78, 122.66, 122.29, 121.94, 53.87, 31.33, 31.21, 30.74, 30.67, 28.67, 28.19, 28.12, 25.90, 25.81, 21.57, 21.51, 13.03, 12.99. Mol. Wt 983.28, MALDI-TOF 983.298 Anal. Calcd for C<sub>67</sub>H<sub>70</sub>N<sub>2</sub>O<sub>5</sub>, C, 81.84; H, 7.18; N, 2.85; Found C, 81.81; H, 7.20; N, 2.86.

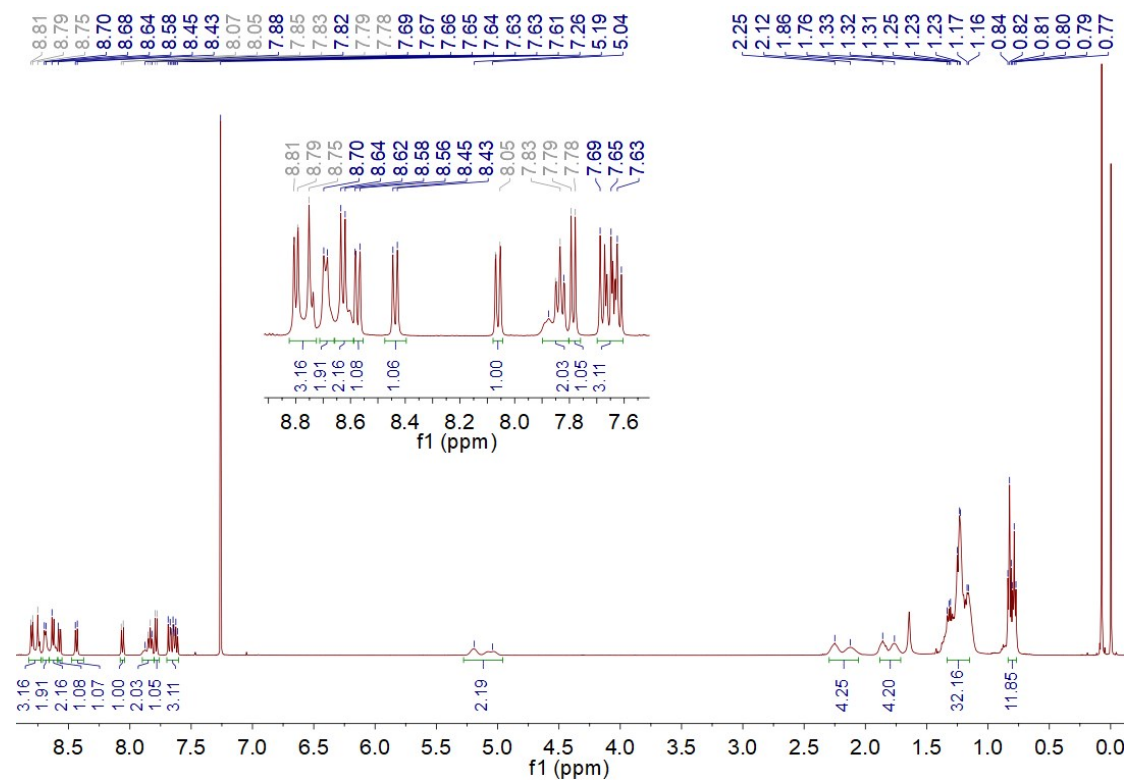


Figure S1 <sup>1</sup>H NMR of compound B-PDI-BZAT in CDCl<sub>3</sub>.

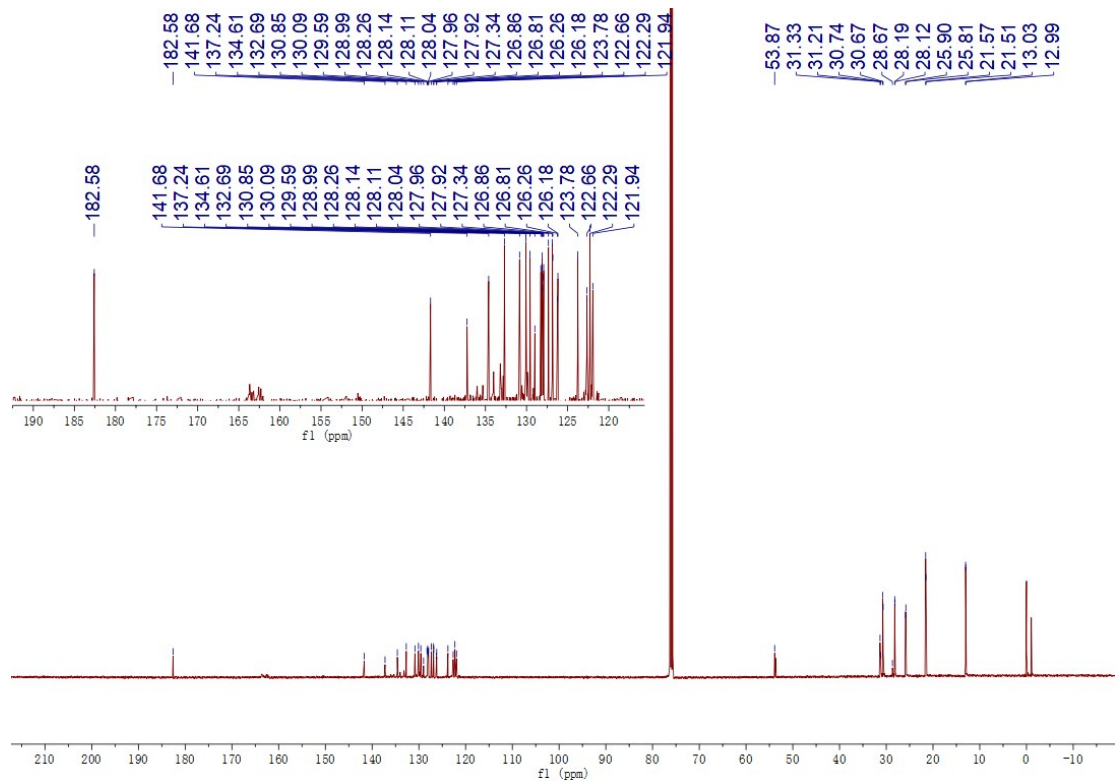


Figure S2  $^{13}\text{C}$  NMR of compound B-PDI-BZAT in  $\text{CDCl}_3$ .

#### Synthesis of O-PDI-BZAT

A mixture of 1 (0.59 g, 1.66 mmol), 3 (0.69 g, 0.83 mmol),  $\text{Pd}(\text{PPh}_3)_4$  (0.05 g, 0.04 mmol),  $\text{K}_2\text{CO}_3$  (0.23 g, 1.66 mmol), DMF (30 mL) was stirred at 80°C under  $\text{N}_2$  atmosphere for 24h. After cooling, DMF was removed by rotary evaporator. The residue was then purified by silica gel column chromatography (petroleum ether: DCM=6:1 to 1:1). A dark red solid of O-PDI-BZAT (0.20 g, 0.2 mmol) was obtained in 25% yield.  $^1\text{H}$  NMR (500MHz,  $\text{CDCl}_3$ )  $\delta$  8.79-8.68 (m, 5H), 8.59-8.50 (m, 5H), 8.38-8.37 (d, 1H), 7.90-7.88 (d, 1H), 7.78-7.75 (t, 1H), 7.69-7.67 (d, 1H), 7.62-7.53 (m, 2H), 5.19 (s, 1H), 4.79 (m, 1H), 2.25 (s, 2H), 1.87 (s, 2H), 1.73 (s, 4H), 1.33-1.21 (m, 32H), 0.83-0.81 (m, 12H).  $^{13}\text{C}$  NMR (125 MHz,  $\text{CDCl}_3$ )  $\delta$  183.88, 163.52, 142.92, 136.19, 134.56, 133.45, 132.03, 131.04, 130.93, 130.30, 129.79, 129.50, 128.99, 128.37, 128.12, 128.00, 127.60, 126.71, 126.47, 124.03, 123.44, 123.30, 123.24, 123.06, 54.82, 31.75, 31.44, 30.19, 29.70, 29.21, 26.94, 22.58, 14.04. Mol. Wt 983.28, MALDI-TOF 983.387 Anal. Calcd for  $\text{C}_{67}\text{H}_{70}\text{N}_2\text{O}_5$ , C, 81.84; H, 7.18; N, 2.85; Found C, 81.79; H, 7.19; N, 2.88.

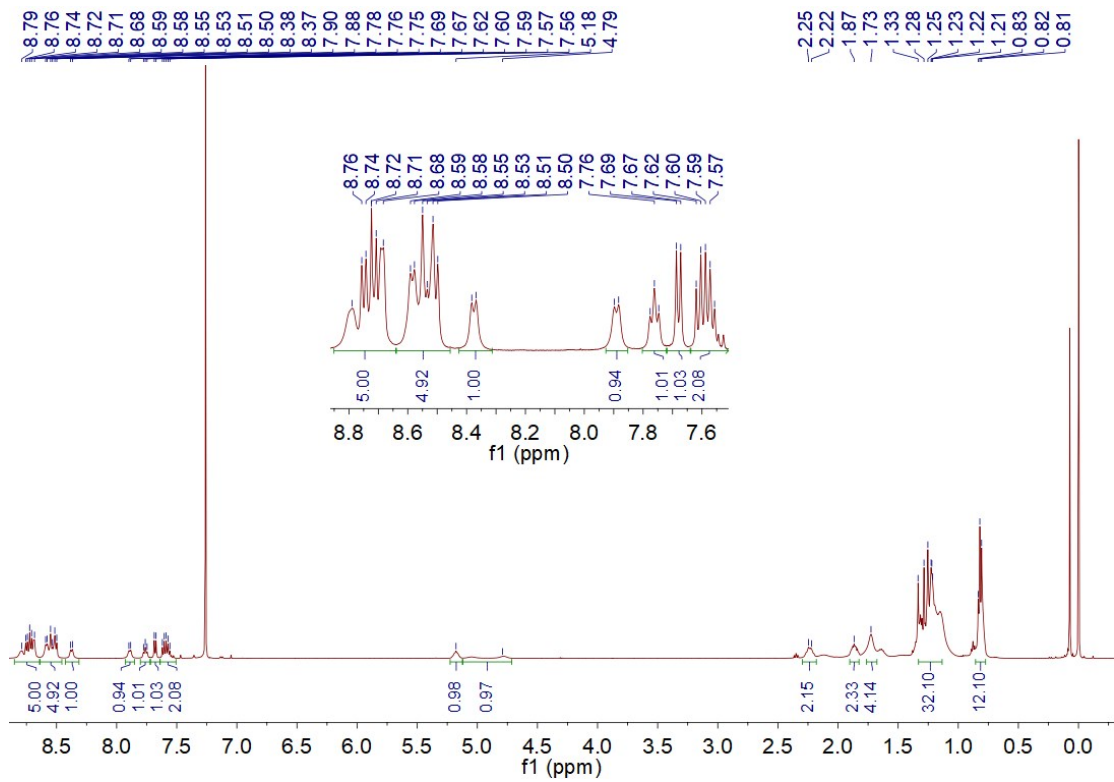


Figure S3  $^1\text{H}$  NMR of compound O-PDI-BZAT in  $\text{CDCl}_3$ .

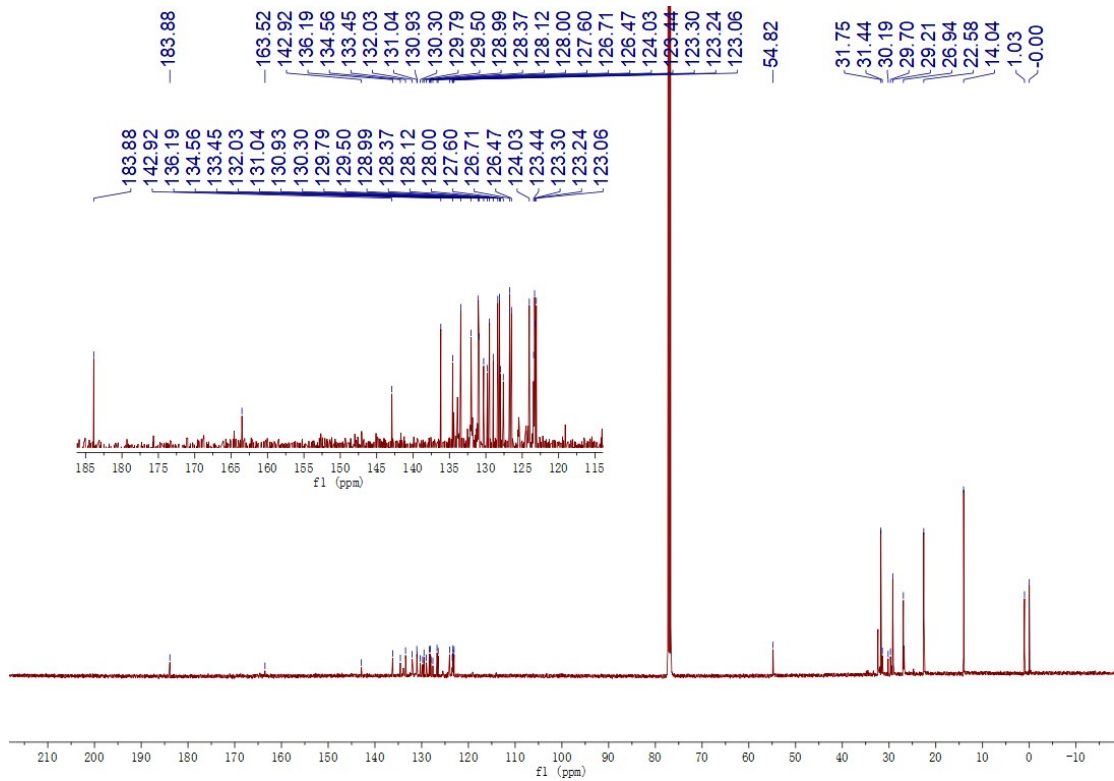


Figure S4  $^{13}\text{C}$  NMR of compound O-PDI-BZAT in  $\text{CDCl}_3$ .

## 2. Femtosecond and Nanosecond Transient Absorption experiments

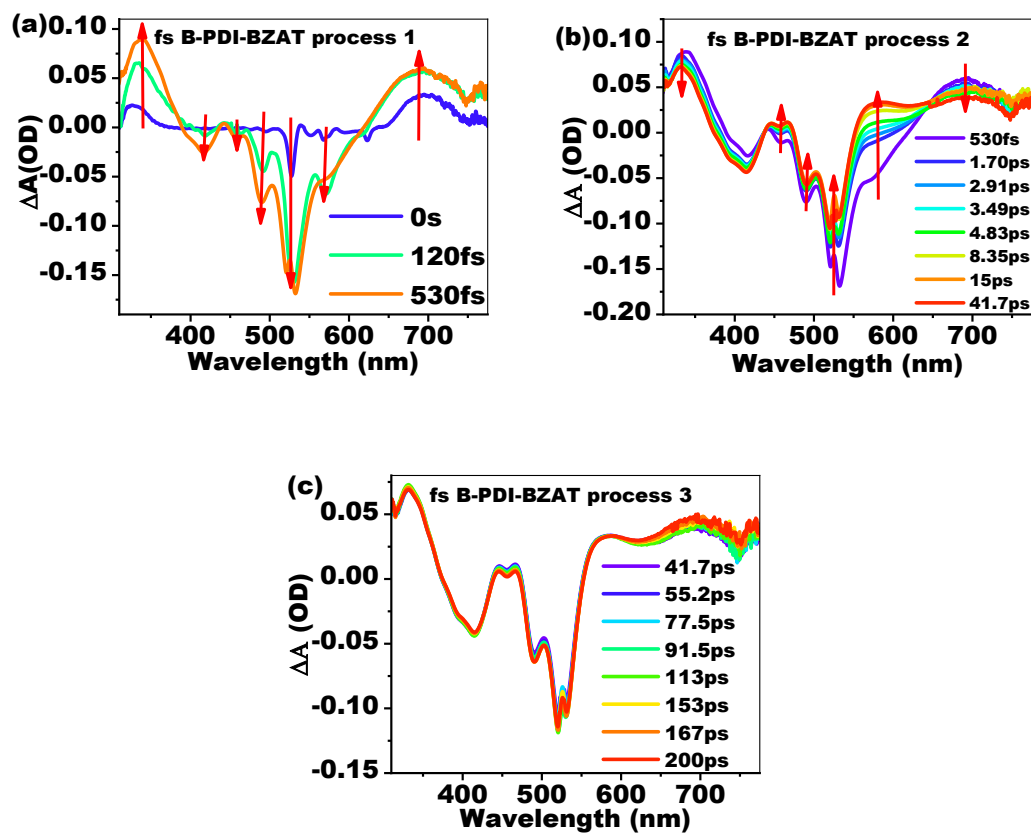


Figure S5 Parts of the fs-TA spectra of B-PDI-BZAT

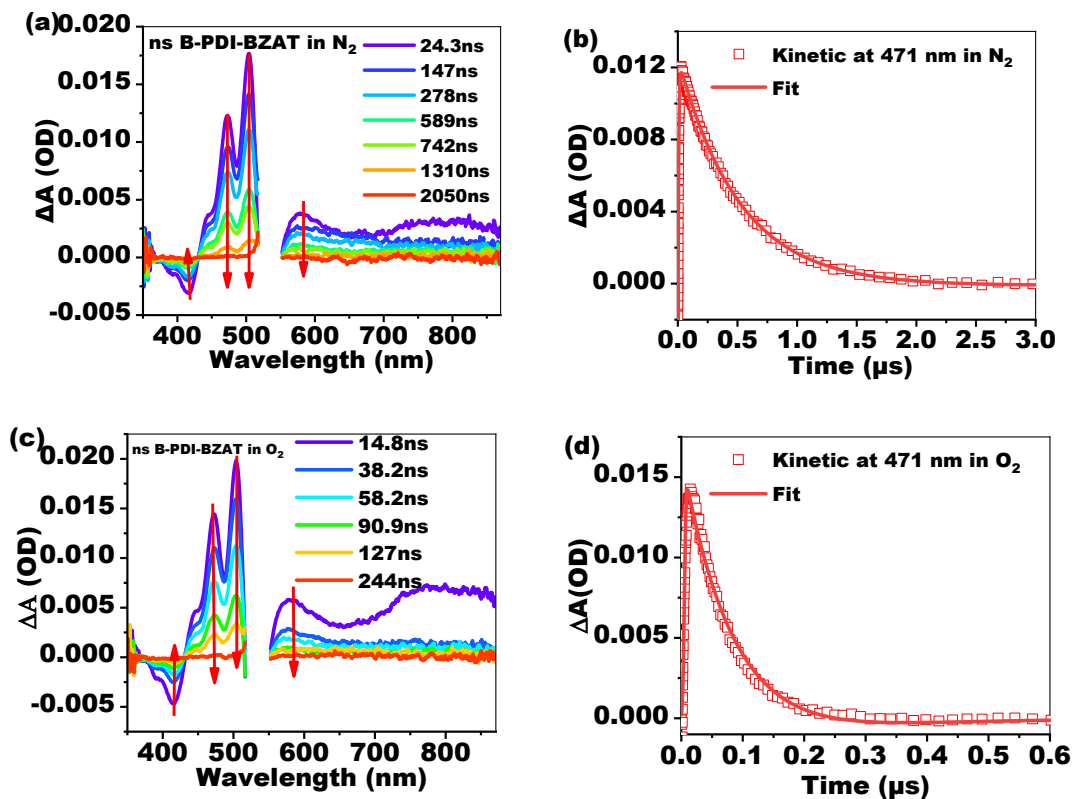


Figure S6 Ns-TA spectra and kinetics of B-PDI-BZAT in THF purged with N<sub>2</sub> or O<sub>2</sub>

Table S1 Kinetic fitting decay lifetimes of the corresponding wavelengths for B-PDI-BZAT measured by fs-TA and ns-TA (in N<sub>2</sub> and O<sub>2</sub>)

	$\lambda$ (nm)	A <sub>1</sub>	$\tau_1$	A <sub>2</sub>	$\tau_2$	A <sub>3</sub>	$\tau_3$	A <sub>4</sub>	$\tau_4$
Fs	491	0.105	0.437ps	0.0634	3.68p	0.135	280p	0.548	7260p
					S		S		S
Ns in N <sub>2</sub>	471	0.366	0.511us						
Ns in O <sub>2</sub>	471	0.5	0.108us						

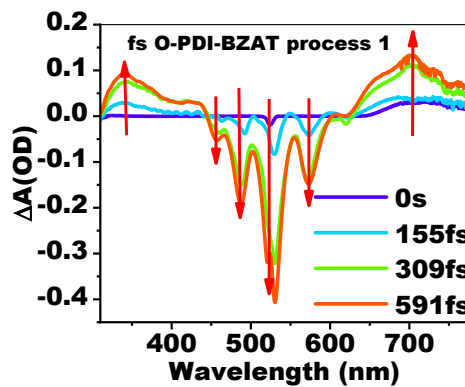


Figure S7 Parts of the fs-TA spectra of O-PDI-BZAT

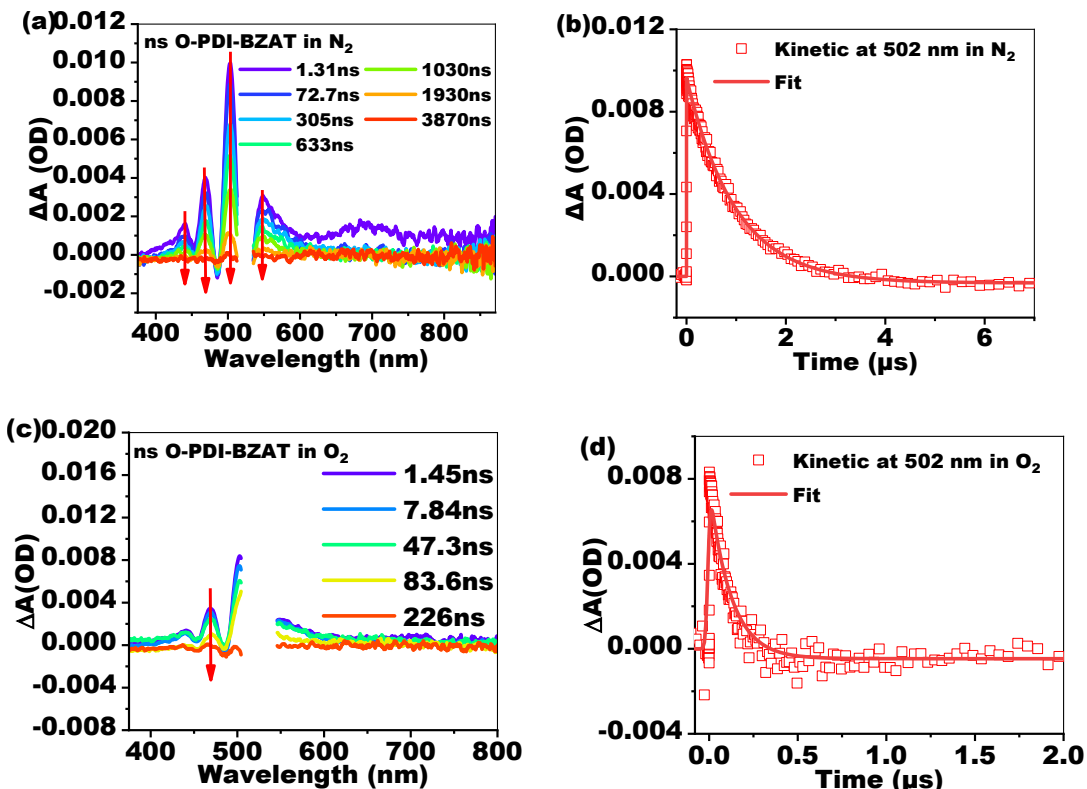


Figure S8 Ns-TA spectra and kinetics of O-PDI-BZAT in THF purged with N<sub>2</sub> or O<sub>2</sub>

Table S2 Kinetic fitting decay lifetimes of the corresponding wavelengths for O-PDI-BZAT measured by fs-TA and ns-TA (in N<sub>2</sub> and O<sub>2</sub>)

	$\lambda(\text{nm})$	A1	$\tau_1$	A2	$\tau_2$	A3	$\tau_3$	A4	$\tau_4$
Fs	502	0.125	0.118ps	0.213	3.09p	0.474	13.4p	0.0434	147p
					s		s		s
Ns in N <sub>2</sub>	502	0.969	0.979us						
Ns in O <sub>2</sub>	502	0.949	0.121us						

Figure S6 shows that the signals (471 and 505 nm) generated by ISC are gradually decreased to the baseline from 24.3 ns to 2.05  $\mu\text{s}$ . The kinetic fitting at 471 nm shows that B-PDI-BZAT has a long lifetime of  $\tau_1 = 0.511 \mu\text{s}$ . When the solution is purged with oxygen, the long-lifetime transient state is significantly quenched by the oxygen and the lifetime drops down to 0.108  $\mu\text{s}$ . This demonstrates that the long-lifetime transient state with main peaks at 471 and 505 nm of B-PDI-BZAT has a triplet-state nature. Similar ns-TA quenching results are also observed for O-PDI-BZAT (Figure S8). The major triplet state located at 469 and 502 nm gradually decay with a lifetime of 0.979  $\mu\text{s}$  in a nitrogen-saturated solution and with a much shorter lifetime of 0.121  $\mu\text{s}$  in an oxygen-saturated solution.

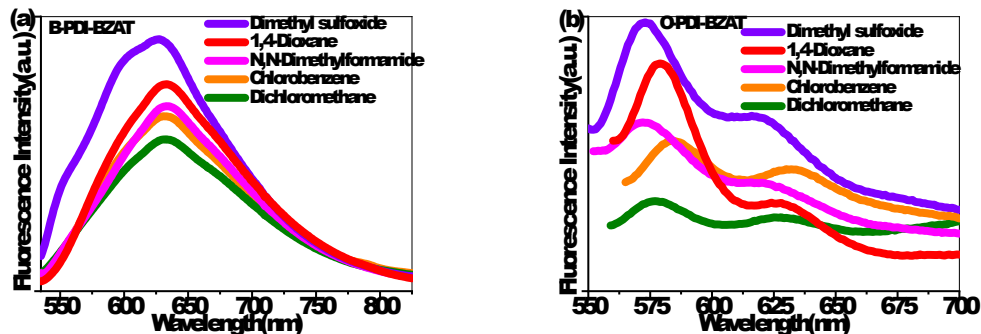


Figure S9 The fluorescence emission behaviors of B-PDI-BZAT (a) and O-PDI-BZAT (b) in five good solvents with different viscosities. The excitation wavelength of fluorescence emission spectra for B-PDI-BZAT and O-PDI-BZAT is 525 nm

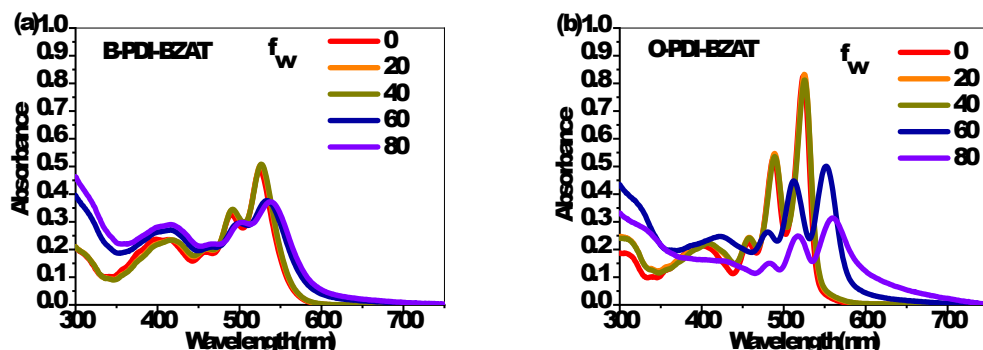


Figure S10 The UV-vis absorption changes of B-PDI-BZAT (a) and O-PDI-BZAT (b) upon the addition of non-solvent water

#### References

1. (a) Cao, L.; Zhang, D.; Xu, L.; Fang, Z.; Jiang, X.-F.; Lu, F., Perylenediimide–Benzanthrone Dyad: Organic Chromophores with Enhanced Third-Order Nonlinear-Optical Activities. *European Journal of Organic Chemistry* **2017**, 2017 (17), 2495-2500; (b) Holman, M. W.; Liu, R.; Adams, D. M., Single-Molecule Spectroscopy of Interfacial Electron Transfer. *Journal of the American Chemical Society* **2003**, 125 (41), 12649-12654; (c) Davis, N. J. L. K.; MacQueen, R. W.; Roberts, D. A.; Danos, A.; Dehn, S.; Perrier, S.; Schmidt, T. W., Energy transfer in pendant perylene diimide copolymers. *Journal of Materials Chemistry C* **2016**, 4 (35), 8270-8275; (d) Horinouchi, H.; Sakai, H.; Araki, Y.; Sakanoue, T.; Takenobu, T.; Wada, T.; Tkachenko, N. V.; Hasobe, T., Controllable Electronic Structures and Photoinduced Processes of Bay-Linked Perylenediimide Dimers and a Ferrocene-Linked Triad. *Chemistry – A European Journal* **2016**, 22 (28), 9631-9641; (e) Teraoka, T.; Hiroto, S.; Shinokubo, H., Iridium-Catalyzed Direct Tetraarylation of Perylene Bisimides. *Organic Letters* **2011**, 13 (10), 2532-2535; (f) Han, H.; Ma, L.-K.; Zhang, L.; Guo, Y.; Li, Y.; Yu, H.; Ma, W.; Yan, H.; Zhao, D., Tweaking the Molecular Geometry of a Tetraperylenediimide Acceptor. *ACS Applied Materials & Interfaces* **2019**, 11 (7), 6970-6977.